Preferential Locations of Polypoidal Lesions and Adjacent Pigment Epithelium Detachments in Polypoidal Choroidal Vasculopathy in a Japanese Population

Takahiro Kogo, Yuki Muraoka, Masayuki Hata, Masaharu Ishikura, Naomi Nishigori, Yuki Akiyama, Naoko Ueda-Arakawa, Manabu Miyata, Sotaro Ooto, Ayako Takahashi, Masahiro Miyake, and Akitaka Tsujikawa

Department of Ophthalmology and Visual Sciences, Kyoto University Graduate School of Medicine, Kyoto, Japan

Correspondence: Yuki Muraoka, Department of Ophthalmology and Visual Sciences, Kyoto University Graduate School of Medicine, 54 Shogoin Kawahara-cho, Sakyo-ku, Kyoto 606-8507, Japan; muraoka@kuhp.kyoto-u.ac.jp.

Received: September 13, 2024
Accepted: February 9, 2025
Published: February 28, 2025

Citation: Kogo T, Muraoka Y, Hata M, et al. Preferential locations of polypoidal lesions and adjacent pigment epithelium detachments in polypoidal choroidal vasculopathy in a Japanese population. *Invest Ophthalmol Vis Sci.* 2025;66(2):70. https://doi.org/10.1167/iovs.66.2.70

Purpose. To analyze the relationship between neovascular lesions in polypoidal choroidal vasculopathy (PCV) and vortex vein characteristics.

Methods. Eighty eyes from 77 patients with PCV were examined using widefield swept-source optical coherence tomography (OCT) and indocyanine green angiography. Polypoidal lesions and pigment epithelial detachments (PEDs) were mapped onto choroidal en face OCT images. Vortex vein drainage areas were assessed for vertical asymmetry, and their associations with lesion locations were analyzed. Choroidal thickness was measured centrally and peripherally. Eyes were classified as pachychoroid or non-pachychoroid.

Results. Thirty-nine eyes (49%) and 41 eyes (51%) were included in the pachychoroid and non-pachychoroid groups, respectively. In total, 95 polypoidal lesions and 80 PEDs were identified. Significant clustering of polypoidal lesions and PEDs was observed near the upstream ends of the vortex veins ($P < 0.001$ for both), particularly in eyes with asymmetric vortex veins; however, no lesions were observed on the non-dominant side. Compared to the pachychoroid group, the non-pachychoroid group exhibited a higher number of soft drusen ($P = 0.026$) and lower central and peripheral choroidal thicknesses ($P < 0.001$ for both), along with less frequent Haller vessel dilation and choroidal vascular hyperpermeability ($P < 0.001$ for both).

Conclusions. The distribution of polypoidal lesions and PEDs in PCV eyes suggests that vortex vein abnormalities may contribute to its pathogenesis. Differences between pachychoroid and non-pachychoroid groups indicate distinct underlying pathologies. Assessing lesion locations relative to vortex veins may improve our understanding of PCV pathology and guide tailored treatments.

Keywords: polypoidal choroidal vasculopathy, vortex vein, pachychoroid

Polypoidal choroidal vasculopathy (PCV), defined by polypoidal lesions at the margins of a branching neovascular network, is widely recognized as a subtype of neovascular age-related macular degeneration (AMD).[1,2] Neovascular AMD, often associated with drusen, has traditionally been considered as a condition primarily affecting the macula, as its name implies. Recent advances in chorioretinal imaging, particularly enhanced depth imaging (EDI) in widefield swept-source optical coherence tomography (SS-OCT), have revealed that many patients with PCV exhibit a pachychoroid phenotype.[3–9] Photodynamic therapy has proven highly effective for pachychoroid PCV, underscoring the importance of understanding its pathogenesis and ensuring accurate diagnosis to guide treatment.[9,10] The pachychoroid spectrum includes conditions characterized by increased choroidal thickness and associated abnormalities. Emerging evidence links vortex vein blood flow disturbances to pachychoroid spectrum diseases pathogenesis.[4,11–17]

Lesion localization in pachychoroid spectrum diseases has been investigated to better understand these conditions. In central serous chorioretinopathy (CSC), a typical pachychoroid spectrum disease, pigment epithelial detachment (PED) and leak points frequently occur around the upstream ends (the macular side) of the vortex veins.[17] Similarly, macular neovascularization (MNV) in pachychoroid neovasculopathy often develops at anastomoses between superior and inferior vortex veins.[18] However, the role of vortex vein characteristics in PCV pathogenesis remains unclear. This study analyzed EDI widefield SS-OCT chorioretinal data from PCV-affected eyes to explore the relationship between vortex vein characteristics and PCV pathologies. Insights gained may enhance our understanding of PCV pathogenesis and guide therapeutic approaches.

Methods

Participants

This observational study, approved by the Institutional Review Board of Kyoto University Graduate School of Medicine, was conducted in accordance with the tenets of the Declaration of Helsinki. Written informed consent was obtained from each patient prior to any procedures or examinations. The study included consecutive patients with PCV who visited the Department of Ophthalmology and Visual Sciences at Kyoto University Hospital between November 2021 and January 2024. Patients had not received any previous treatments, such as laser coagulation or photodynamic therapy, that could alter vortex vein characteristics. PCV diagnosis was based on the presence of branching vascular networks with polypoidal vascular dilation on indocyanine green angiography (ICGA) and elevated lesions observed on OCT B-scan images.

Exclusion criteria included other chorioretinal diseases, retinal circulatory diseases, inferior posterior staphyloma, pit macular syndrome, uveitis, scleritis, ocular hypertension (>21 mmHg), ocular hypotension (<5 mmHg), a history of intraocular surgery (except cataract surgery), corticosteroid use, or anti-vascular endothelial growth factor therapy within the last month. Additional exclusions were made for patients with keratoconus, high myopia (spherical equivalent <−6 D), hyperopia (>+4 D), astigmatism (>±3 D), pregnancy, or low-quality OCT images (signal strength index <5) due to eye movement or media opacities.

During the initial consultation, each patient underwent a comprehensive ophthalmic evaluation, including refraction, measurement of decimal best-corrected visual acuity (BCVA) using the 5-meter Landolt chart, intraocular pressure measurements, axial length measurement, slit-lamp biomicroscopy, color fundus photography, fluorescein angiography (FA), ICGA, fundus autofluorescence photography, and SS-OCT. Refractive error was measured using an autorefractor (ARK-530A; NIDEK, Gamagori, Japan). The spherical equivalent was calculated as the sum of the spherical power and half of the cylindrical power. Axial length was measured using an interferometer (IOLMaster 700; Carl Zeiss Meditec, Dublin, CA, USA). Color fundus photographs were captured with a dedicated fundus camera (TRC50LX; Topcon Corporation, Tokyo, Japan), and FA and ICGA were performed using a 55°-span confocal scanning laser ophthalmoscope (SPECTRALIS HRA+OCT; Heidelberg Engineering, Heidelberg, Germany).

Evaluation of Choroidal Thickness Using EDI in Widefield SS-OCT

Chorioretinal structures were evaluated using an SS-OCT system (Xephilio OCT-S1; Canon, Tokyo, Japan) with an illumination range of 1010 to 1110 nm and a scanning speed of 100,000 A-scans per second. The OCT focusing spot was set at 30 µm to achieve broader scan coverage without supplementary lenses or device alterations. This setting reduces the beam diameter, increasing the variation in the angle of incidence of the observation light, which enables expansive coverage. At the same time, it maintains sufficient resolution for detailed observation.

To measure choroidal thickness in the posterior pole, three-dimensional volume data were obtained over a 20-mm (vertical, 128 B-scans) × 23-mm (horizontal, 1024 pixels) × 5.3-mm (scan depth, 1396 pixels) area of the posterior pole using EDI in SS-OCT. Choroidal thickness maps were analyzed using our previously reported method.[16,19,20] A grid with 3-, 9-, and 18-mm-diameter circles was centered on the fovea. The middle (3–9 mm) and peripheral (9–18 mm) rings were subdivided into quadrants: superotemporal, inferotemporal, superonasal, and inferonasal, resulting in nine subfields, including the macular 3-mm ring (Fig. 1).

Detection of PED Using Choroidal En Face Images Obtained from EDI in Widefield SS-OCT

To create maps of PED and choroidal en face images, three-dimensional volume data were acquired over a 20-mm (vertical, 512 pixels) × 23-mm (horizontal, 512 B-scans) × 5.3-mm (depth, 1396 pixels) area, similar to the previous section. The PED layer was defined as the space between the outer surface of the retinal pigment epithelium (RPE), approximately corresponding to the RPE basal lamina, and Bruch's membrane, approximately corresponding to the inner collagenous layer of Bruch's membrane, whereas the choroid was defined as the area between Bruch's membrane and the chorioscleral boundary (Fig. 2). To evaluate fibrovascular PEDs, including regions with double-layer signs, we assessed only PEDs contiguous with polypoidal lesions. Areas identified as serous, hemorrhagic, or drusenoid PEDs were excluded based on multimodal imaging, including fundus photographs, OCT findings, and FA. Scan noise was removed using the *erode* and *dilate* functions of ImageJ 1.51 (National Institutes of Health, Bethesda, MD, USA). Segmentation was performed using the artificial intelligence-based function in the Canon Xephilio OCT-S1 system. All B-scan images were reviewed, and any misaligned segmentation was manually corrected based on anatomical landmarks, such as the outer surface of the RPE, Bruch's membrane, and the chorioscleral boundary, using the embedded software.

Location of Polypoidal Lesions and PEDs

Polypoidal lesions were identified as polypoidal vessel dilations during ICGA, which appeared as sharply elevated lesions on OCT B-scan images. The centers of these lesions were defined as their locations. To map lesion locations, we superimposed them on choroidal en face images (Fig. 2) using ImageJ software. All of the PEDs were evaluated during the subjective measurements. However, it was difficult to accurately determine the centers of large PEDs during the objective assessments because of their sizes and irregular shapes (Supplementary Fig. S1). Therefore, in the objective assessments, only PEDs smaller than the area of the optic disc were included. The centers of these PEDs were automatically identified as centroids using ImageJ software.

We objectively assessed the distance and relative positional relationships of the polypoidal lesions and PEDs to the fovea. Given that the distribution of these lesions and their relationship with vortex vein drainage areas may reflect the pathogenesis of pachychoroid spectrum diseases, we subjectively evaluated their locations to determine whether they were within the superior or inferior vortex vein drainage areas, as per a previous study.[17] Areas that could not be

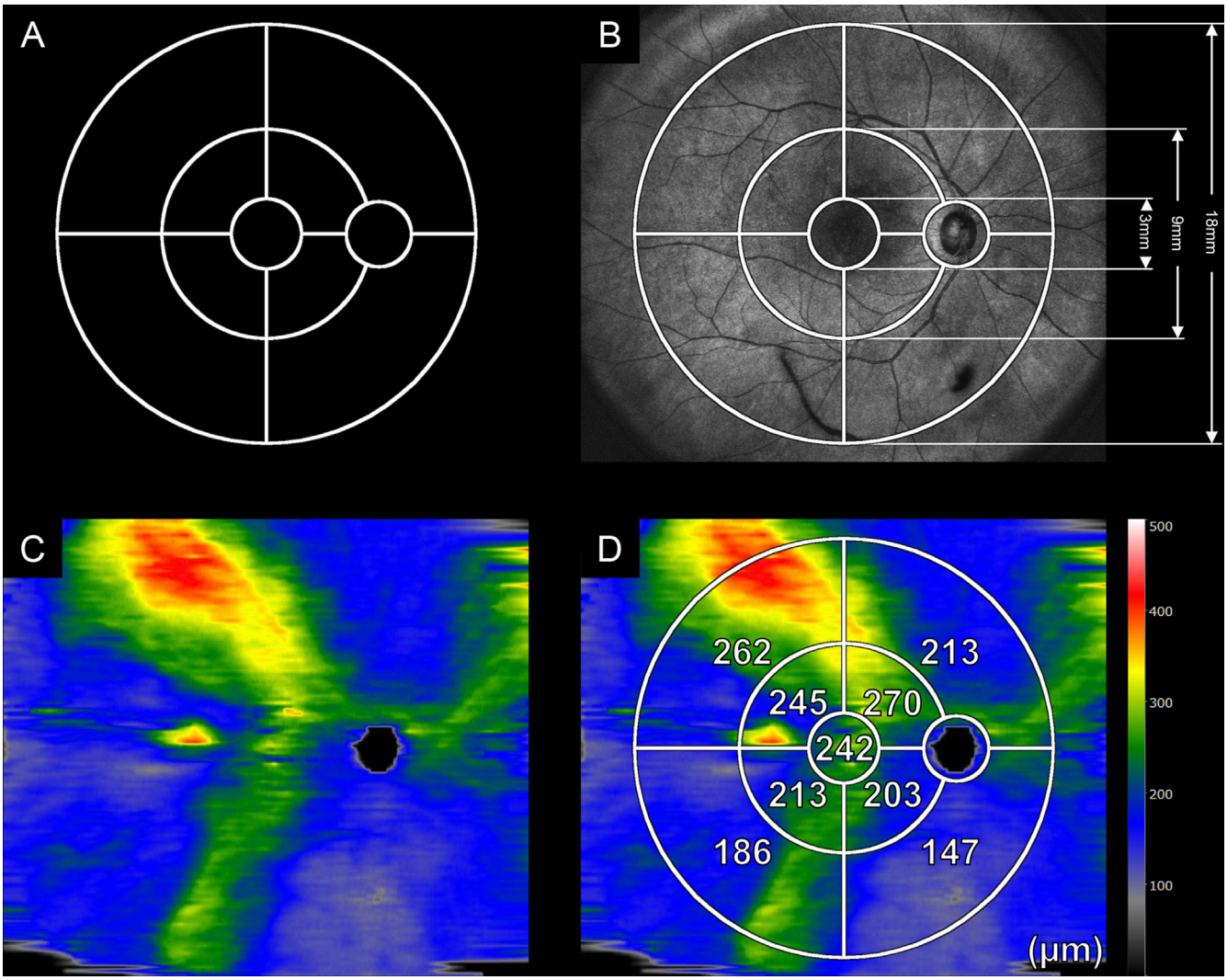

Figure 1. Choroidal thickness map analysis using EDI widefield SS-OCT. (**A**) Grid for measuring widefield choroidal thickness changes, comprised of nine subfields divided by three circles (diameters: 3 mm, 9 mm, and 18 mm) and four lines. Subfields were categorized as superotemporal, inferotemporal, superonasal, or inferonasal based on vortex vein arrangement. (**B**) Infrared scanning laser ophthalmoscopy images overlaid with the measurement grid. (**C**) Choroidal thickness map. (**D**) Mean choroidal thickness values (μm) for each subfield, as measured using the grid.

distinctly assigned were classified as the border zone. Additionally, based on the methodologies of previous studies,[16,21] we evaluated the symmetry between the superior and inferior vortex veins using en face OCT. In eyes with asymmetric vortex veins, the drainage area of vortex veins that crossed the fovea and extended to the opposite side was defined as the dominant side, whereas the other drainage area was termed the non-dominant side, in accordance with the method described in a previous report.[21] The lesion locations were further categorized as most upstream or mid-/downstream based on vortex vein drainage. The ampullary region, where blood exits the eye, was designated as the downstream endpoint; the upstream regions extended toward the macula and included the tips of the medium and large choroidal vessels. The PEDs that overlapped with the upstream ends (tips on the macular side) of a vortex vein were classified as being in the most upstream drainage area, whereas those that did not overlap were classified as PEDs in the mid-/downstream drainage areas. The polypoidal lesions that were located within 1 optic disc diameter of the upstream ends of vortex veins were classified as being in the most upstream drainage area, whereas the others were classified as polypoidal lesions in the mid-/downstream drainage areas.

For standardization, eyes with MNV in the inferior vortex vein drainage area were flipped vertically in en face images. This adjustment ensured that all lesions appeared consistently within the superior vortex vein drainage area, facilitating an objective assessment of their relative positions with respect to the macula and optic disc in the drainage areas.

We comprehensively and objectively evaluated the locations of the polypoidal lesions and PEDs by adopting the segmentation approach used in previous studies.[18,22] The area was partitioned into four sections using the optic disc–fovea line and a vertical line that passed through the optic disc, which served as the boundary lines for the vortex veins.[18,22] The distances of the polypoidal lesions and PEDs

Investigative Ophthalmology & Visual Science

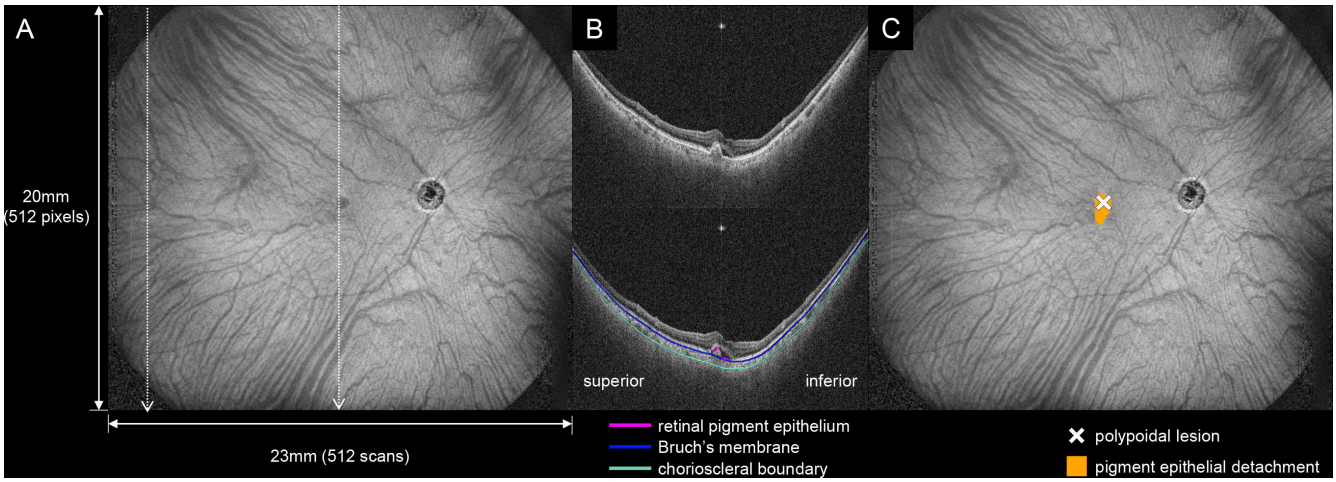

Figure 2. Identification of the locations of polypoidal lesions and adjacent PEDs in PCV. (**A**) En face image of the choroid with a scanning area of 20 mm vertically (512 pixels) × 23 mm horizontally (512 scans). (**B**) The PED layer was defined as the space between the outer surface of the RPE and Bruch's membrane; the choroid lies between Bruch's membrane and the chorioscleral boundary. (**C**) The location of a polypoidal lesion identified using OCT B-scan and ICGA images. The locations of the polypoidal lesion (*white cross*) and the adjacent PED (*orange*) are projected onto the corresponding choroidal en face image.

located in the downstream segment of the vortex vein drainage area relative to the disc–fovea line were measured from the disc–fovea line. To determine the distances from the polypoidal lesions and PEDs and both the fovea and disc–fovea lines, we employed the Bennett formula, a modified version of the Littmann formula, adjusting for magnification related to axial length.[23,24]

Classification of Pachychoroid and Non-Pachychoroid Groups

Based on previous studies,[9] eyes were classified into pachychoroid and non-pachychoroid groups. Pachychoroid eyes met all three criteria: absence of drusen (except pachydrusen), focal choroidal vascular hyperpermeability (CVH) on late-phase ICGA, and dilated outer choroidal vessels on OCT B-scan images. Drusen were classified based on previous reports, with pachydrusen defined as isolated or scattered yellow–white deposits > 63 µm in diameter.[25,26] The subjective lesion location evaluations and the classification were independently assessed by two retinal specialists (TK, NN) to ensure objectivity. Discrepancies were resolved by consultation with a third specialist (YM) if necessary.

Statistical Analysis

Data were analyzed using JMP Pro 16.0 (SAS Institute, Cary, NC, USA). Values are expressed as mean ± SD. BCVA was converted to logarithm of the minimum angle of resolution (logMAR) equivalents. Fisher's exact test identified areas with the highest number of polypoidal lesions and PEDs, sex and asymmetry differences between groups, and distribution differences of lesions in eyes with and without asymmetric vortex veins. The Mann–Whitney *U* test was used for continuous variable comparisons between groups. Multiple linear regression adjusted for age, sex, and axial length was used to compare choroidal thickness. The Wilcoxon signed-rank test assessed differences in lesion distribution. Significance was defined as $P < 0.05$.

Results

Patient Demographics and Lesion Characteristics

We analyzed 80 eyes from 77 patients with PCV, including 54 males and 23 females (Table 1). Each eye exhibited polypoidal lesions associated with a single PED. A total of 95 polypoidal lesions and 80 PEDs were identified. The PED areas varied significantly, ranging from 0.6 to 56.3 mm^2, with a mean of 6.1 ± 7.4 mm^2. The largest PED exceeded 10 times the disc area (Supplementary Fig. S1). Among the eyes analyzed, five eyes (6%) demonstrated peripapillary PCV.

Lesion Distributions Relative to the Fovea

Figure 3 illustrates the spatial distributions of polypoidal lesions and PEDs. The frequency of both polypoidal lesions and PEDs decreased with increasing distance from the fovea. Notably, 48% of the polypoidal lesions and 60% of the PEDs were located within 1 mm of the fovea. Polypoidal lesions and PEDs were observed nasal to the fovea in 69% and 70% of the eyes, respectively, and were significantly more frequent in the nasal than in the temporal region ($P < 0.001$ for both). Additionally, horizontal distances from the fovea along the disc–fovea line were significantly greater than vertical distances for both lesion types (polypoidal lesions: horizontal = 1.1 ± 1.0 mm, vertical = 0.8 ± 0.6 mm, $P = 0.008$; PEDs: horizontal = 0.9 ± 0.8 mm, vertical = 0.6 ± 0.3 mm, $P = 0.001$).

Association Between Lesion Locations and Vortex Veins

Of the 80 eyes assessed, 78 (98%) had polypoidal lesions, and 47 (59%) had PEDs in either the superior or inferior vortex vein drainage area (Table 2). Remaining cases involved PEDs spanning both areas or lesions in the border zone. No polypoidal lesions were identified in both vortex vein drainage areas simultaneously. Polypoidal

Investigative Ophthalmology & Visual Science

Table 1. Characteristics of Patients With PCV

Characteristic	Value
Number of patients (men, women)	77 (54, 23)
Number of eyes (men/women)	80 (56, 24)
Age (y), mean ± SD (range)	74.5 ± 9.0 (51–89)
Axial length (mm), mean ± SD (range)	23.8 ± 1.0 (21.6–25.8)
Number of eyes with prior anti-VEGF treatment	10
BCVA (logMAR), mean ± SD (range, Snellen equivalent)	0.30 ± 0.34 (20/667–20/13)
Symptom duration (mo), mean ± SD (range)	21.5 ± 37.1 (0.1–165)
Polypoidal lesions per eye, mean ± SD (range)	1.2 ± 0.4 (1–3)
PEDs contiguous with polypoidal lesions per eye, mean ± SD (range)	1.0 ± 0.0 (1–1)
Area of PED (mm^2), mean ± SD (range)	6.1 ± 7.4 (0.6–56.3)
Ratio of PED area to disc area, mean ± SD (range)	1.4 ± 1.5 (0.2–10.9)

VEGF, vascular endothelial growth factor.

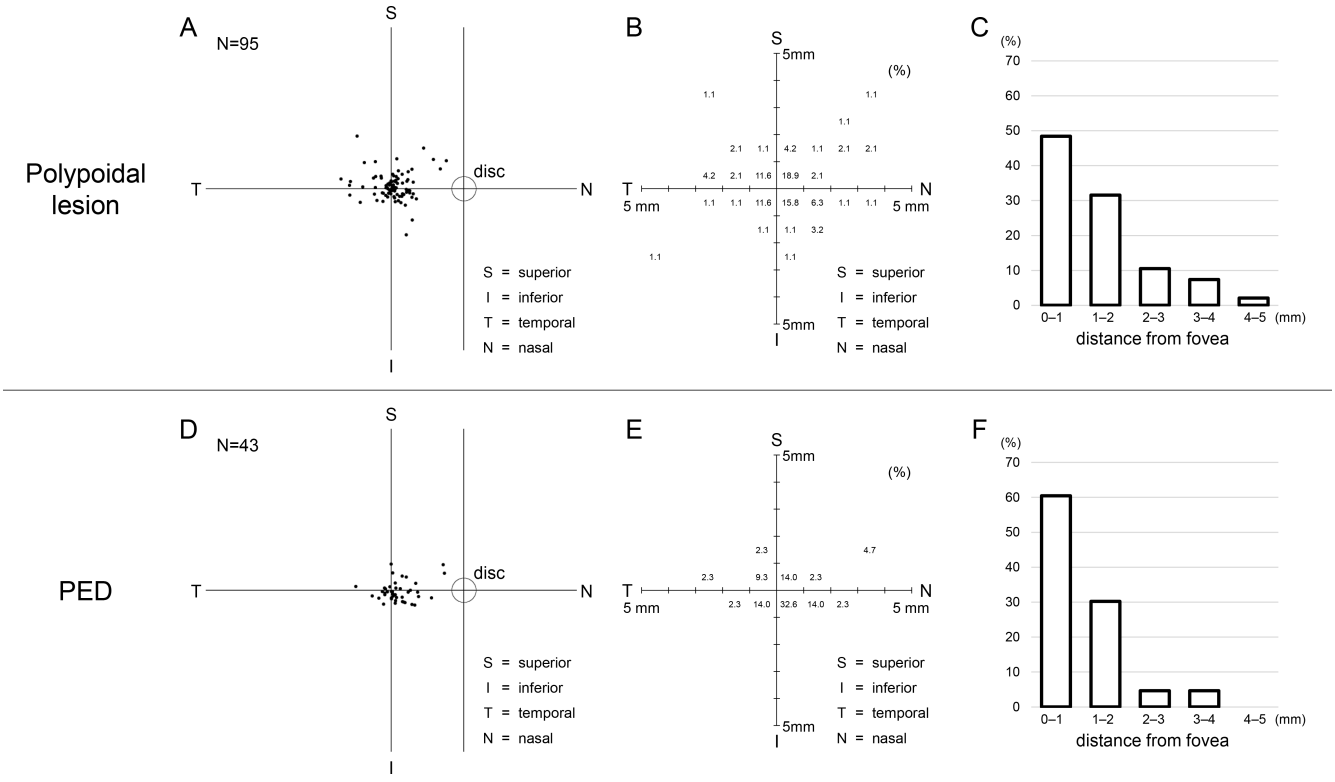

Figure 3. Relative locations of polypoidal lesions and adjacent PEDs to the fovea. (**A**, **D**) Locations of polypoidal lesions (**A**) and PEDs (**D**) relative to the fovea and optic disc. (**B**, **E**) Distribution of distances from the fovea along and perpendicular to the disc–fovea line, showing that polypoidal lesions (**B**) and PEDs (**E**) were predominantly nasal to the fovea in 69% and 70% of eyes, respectively. Both were more frequently located nasally than temporally ($P < 0.001$ for both). Horizontal distances along the disc–fovea line exceeded vertical distances ($P = 0.008$ and $P = 0.001$, respectively). (**C**, **F**) Spatial distributions of polypoidal lesions (**C**) and PEDs (**F**) relative to the fovea, demonstrating a decrease in lesion and PED numbers with increasing distance from the fovea. However, only 48% of polypoidal lesions and 60% of PEDs were located within 1 mm of the fovea.

Table 2. Locations of PEDs and Polypoidal Lesions in Relation to Vortex Vein Characteristics

Total eyes ($n = 80$)	Most Upstream, n	Midstream or Downstream, n	P
Eyes with polypoidal lesions, n	69	12	<0.001
Eyes with PED, n	40	7	<0.001
Eyes with asymmetric vortex veins ($n = 49$)	Dominant Side	Non-Dominant Side	P
Eyes with polypoidal lesions, n	49	0	<0.001
Eyes with PED, n	36	0	<0.001

Comparisons of the presence or absence of polypoidal lesions and PEDs between each domain were performed using Fisher's exact test. Eyes were counted if they had polypoidal lesions of PEDs in each area.

Investigative Ophthalmology & Visual Science

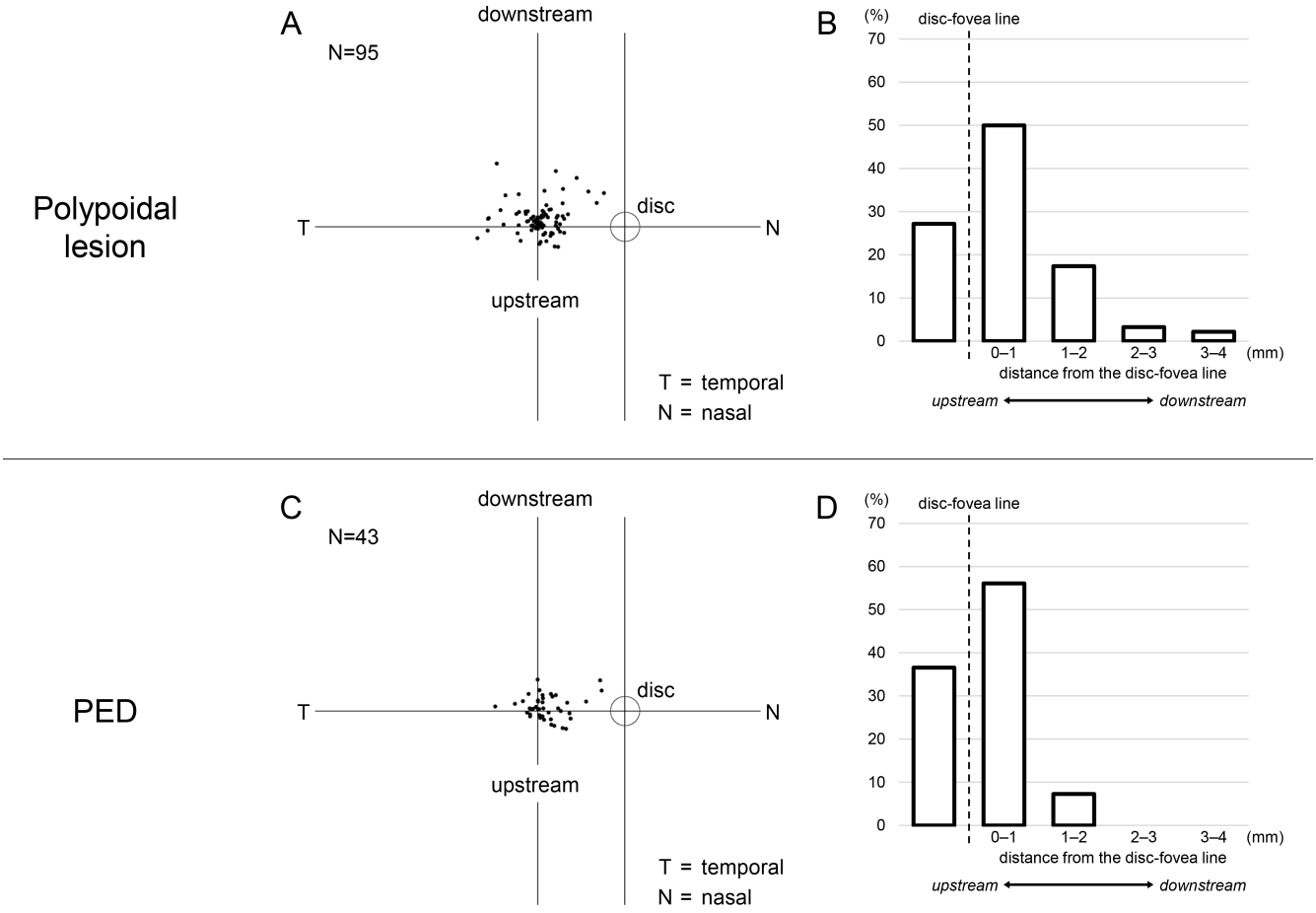

Figure 4. Locations of polypoidal lesions and adjacent PEDs relative to the vortex vein drainage area. (**A**, **C**) Locations of polypoidal lesions (**A**) and PEDs (**C**) relative to the vortex vein drainage area after adjusting the data by converting the position of the inferior vortex vein to correspond to that of the superior vortex vein. Both polypoidal lesions and PEDs exhibited a band-like pattern along the disc–fovea line. (**B**, **D**) Distribution of lesion distances from the disc–fovea line reveals their presence in superior or inferior vortex vein drainage areas. Seventy-seven percent of polypoidal lesions and 93% of PEDs were located near (0–1 mm) or above the disc–fovea line, corresponding to the upstream areas of the vortex veins in many cases.

lesions and PEDs were predominantly located upstream of the vortex vein drainage areas ($P < 0.001$ for both). In eyes with peripapillary PCV, all PEDs and polypoidal lesions were situated at the terminal ends of superior or inferior vortex vein drainage areas or spanned across both regions (Supplementary Table S1). Among the 49 eyes with asymmetric vortex veins, all exhibited polypoidal lesions in the dominant vortex vein area, where dilated vortex veins were often observed. Additionally, 36 eyes (73%) showed PEDs in this dominant area, whereas neither polypoidal lesions nor PEDs were found in non-dominant areas.

Lesion Distributions Relative to Vortex Vein Drainage Areas

Figure 4 demonstrates the distribution of polypoidal lesions and PEDs relative to vortex vein drainage areas. Of the 93 polypoidal lesions (97%) and 41 PEDs (95%) clearly located in either the superior or inferior vortex vein drainage area, most lesions (polypoidal lesions, 77%; PED, 93%) were near (within 0–1 mm) or upstream of the disc–fovea line. Lesions in eyes with asymmetric vortex veins were more distally located than in eyes without asymmetric vortex veins (polypoidal lesions, $P < 0.001$; PEDs, $P = 0.002$) (Fig. 5).

Clinical and Lesion Features of Eyes With Pachychoroid and Non-Pachychoroid PCV

Table 3 compares the clinical features of pachychoroid and non-pachychoroid groups. Pachydrusen were observed in 26% of eyes in the pachychoroid group and 22% in the non-pachychoroid group. Soft drusen were present in 15% of eyes in the non-pachychoroid group. Asymmetric vortex veins were found in 69% of eyes in the pachychoroid group and 54% in the non-pachychoroid eyes. In the non-pachychoroid group, 12% of eyes exhibited dilated Haller vessels, and 29% had CVH, both significantly lower proportions compared to the pachychoroid group ($P < 0.001$ for both). After adjusting for age, sex, and axial length, pachychoroid eyes demonstrated significantly thicker choroids in both central macular and peripheral regions compared to non-pachychoroid eyes ($P < 0.001$ for all).

Both groups showed a significant tendency for polypoidal lesions and PEDs to localize upstream of vortex vein

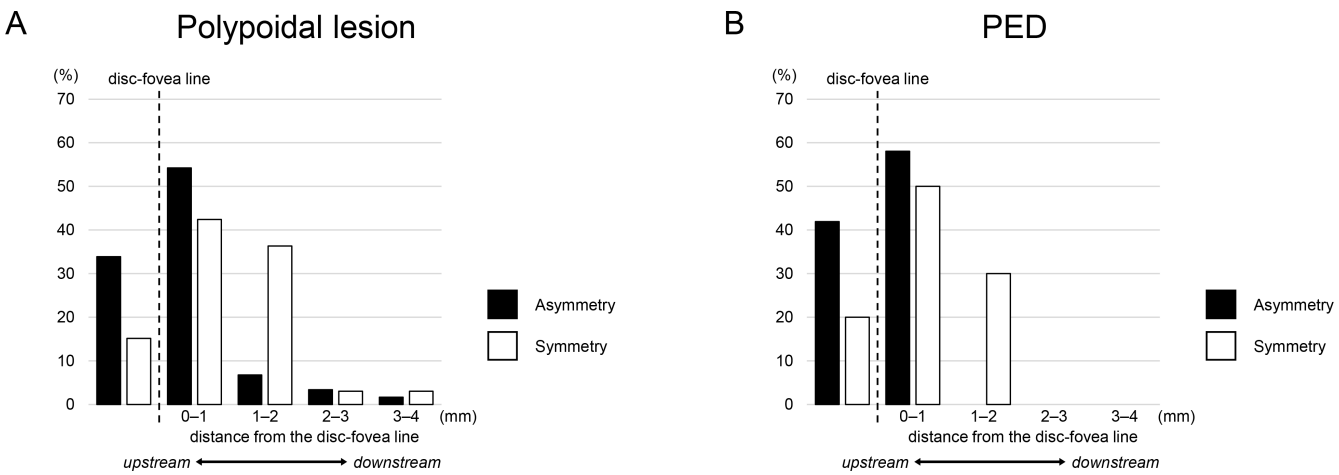

Figure 5. Distribution of polypoidal lesions and adjacent PEDs in relation to vortex vein symmetry. (**A**, **B**) In eyes with asymmetric vortex veins, 88% of polypoidal lesions (**A**) and 100% of PEDs (**B**) were located near (0–1 mm) or upstream of the disc–fovea lines. In eyes without asymmetric vortex veins, 58% of the polypoidal lesions and 70% of PEDs were located near (within 0–1 mm) or upstream of the disc–fovea lines, whereas 36% of the polypoidal lesions and 30% of PEDs were located within 1 to 2 mm of the disc–fovea lines. This difference in distribution was significant (polypoidal lesions, $P < 0.001$; PEDs, $P = 0.002$). Moreover, the polypoidal lesions and PEDs were located distally, which is consistent with the distal positioning of the upstream ends of the vortex veins.

Table 3. Comparison of Clinical Characteristics of Patients With PCV: Pachychoroid Versus Non-Pachychoroid Macular Phenotypes

Characteristic	Pachychoroid ($n = 39$ Eyes)	Non-Pachychoroid ($n = 41$ Eyes)	*P*
Men, women, *n*	28, 11	28, 13	0.810*
Age (y), mean ± SD	72.6 ± 9.7	76.2 ± 8.0	0.112†
Axial length (mm), mean ± SD	23.6 ± 1.0	24.1 ± 0.9	0.012†
BCVA (logMAR), mean ± SD	0.23 ± 0.30	0.37 ± 0.37	0.077†
Symptom duration (mo), mean ± SD	19.6 ± 37.7	23.3 ± 36.9	0.991†
Macular findings, *n* (%)			
Eyes with soft drusen	0 (0)	6 (15)	0.026*
Eyes with hard drusen	0 (0)	13 (32)	<0.001*
Eyes with pachydrusen	10 (26)	9 (22)	0.795*
Eyes with dilated Haller vessels‡	39 (100)	5 (12)	<0.001*
Eyes with CVH	39 (100)	12 (29)	<0.001*
Number of polypoidal lesions per eye, mean ± SD	1.2 ± 0.5	1.1 ± 0.4	0.332†
Area of the PED (mm^2), mean ± SD	5.3 ± 4.7	6.8 ± 9.2	0.610†
Ratio of PED area to disc area, mean ± SD	1.2 ± 1.0	1.6 ± 1.9	0.590†
Eyes with asymmetric vortex veins, *n* (%)	27 (69)	22 (54)	0.175*
Choroidal thickness (μm), mean ± SD			
Macular (0–3 mm in diameter)	309 ± 92	187 ± 48	<0.001†
Middle ring (3–9 mm in diameter)			
Superotemporal	285 ± 82	201 ± 43	<0.001†
Inferotemporal	263 ± 84	179 ± 39	<0.001†
Superonasal	273 ± 87	177 ± 55	<0.001†
Inferonasal	227 ± 96	144 ± 35	<0.001†
Peripheral ring (9–18 mm in diameter)			
Superotemporal	251 ± 59	189 ± 37	<0.001†
Inferotemporal	206 ± 55	157 ± 26	<0.001†
Superonasal	225 ± 69	163 ± 33	<0.001†
Inferonasal	159 ± 60	117 ± 21	<0.001†

* Comparisons of each parameter between the pachychoroid and non-pachychoroid groups were performed using Fisher's exact test.
† Comparisons of each parameter between pachychoroid and non-pachychoroid were performed using the Mann–Whitney *U* test.
‡ Dilation of the Haller vessels was evaluated using macular OCT B-scan images.

drainage areas (pachychoroid group: polypoidal lesions, $P < 0.001$, and PEDs, $P = 0.012$; non-pachychoroid group: polypoidal lesions, $P < 0.001$, and PEDs, $P < 0.001$) (Fig. 6). No significant differences were observed in lesion distributions within vortex vein drainage areas between the two groups (polypoidal lesions, $P = 0.580$; PEDs, $P = 0.223$) (Fig. 7). However, in the non-pachychoroid group, some eyes with soft drusen exhibited polypoidal lesions and PEDs near the fovea, without a specific predilection for the superior or inferior vortex vein drainage areas (Fig. 6).

Investigative Ophthalmology & Visual Science

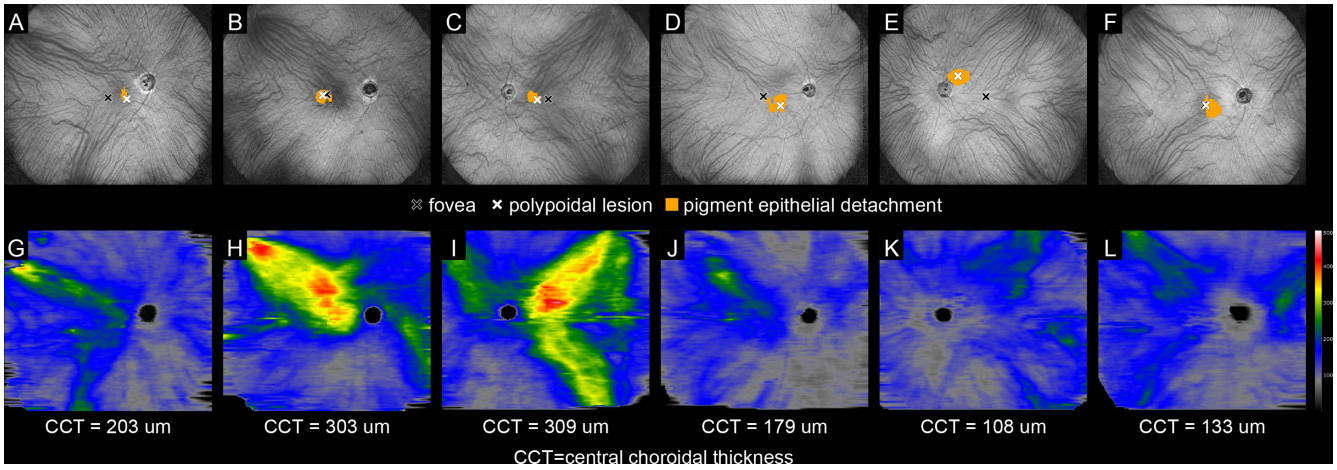

Figure 6. Representative cases of eyes with polypoidal lesions and adjacent pigment epithelial detachments (PEDs). (**A–C**, **G–I**) Pachychoroid group. In most eyes in the pachychoroid group, polypoidal lesions (*white crosses*) and PEDs (*orange*) were located upstream of the superior or inferior vortex veins (**A–C**). In eyes with asymmetric vortex veins, the polypoidal lesions and PEDs tended to occur within the dominant and more dilated vortex vein drainage area. Additionally, choroidal thickening consistent with the course of the vortex veins drainage was often observed, with polypoidal lesions and PEDs frequently occurring upstream (terminal ends) of these veins (**G–I**). (**D–F**, **J–L**) Non-pachychoroid group. In most eyes in the non-pachychoroid group, polypoidal lesions and PEDs were similarly located upstream of the superior or inferior vortex veins (**D**). In cases with asymmetric vortex veins, even with hard drusen or without dilated outer choroidal vessels in the macular area, polypoidal lesions and PEDs often appeared within the vortex vein drainage area on the dominant side. Choroidal thickening in the non-pachychoroid group was less pronounced than in the pachychoroid group (**J**). Similar findings were noted in peripapillary PCV cases (**E**, **K**). However, some eyes with soft drusen demonstrated polypoidal lesions and PEDs near the fovea (*black cross*), without predilection for the superior or inferior vortex vein drainage area (**F**, **L**).

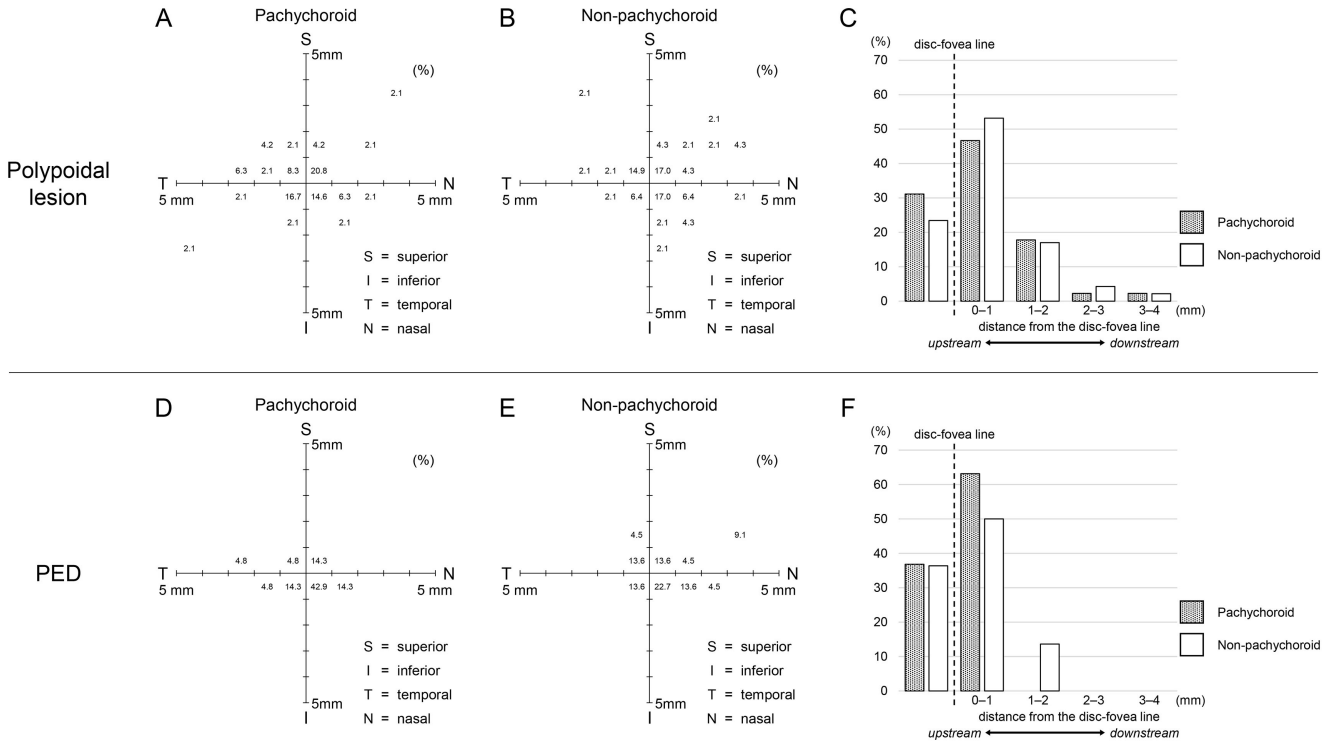

Figure 7. Distribution of polypoidal lesions and adjacent PEDs in the pachychoroid and non-pachychoroid groups. (**A**, **B**, **D**, **E**) Distribution of distances from the fovea along and perpendicular to the disc–fovea line. No significant differences were observed between the groups with regard to the proportion of lesions located within 1 mm of the fovea (polypoidal lesions, $P = 0.949$; PEDs, $P = 0.341$). (**C**, **F**) Distribution of polypoidal lesions (**C**) and adjacent PEDs (**F**) relative to the disc–fovea line in the vortex vein drainage area. In the pachychoroid group, 78% of the polypoidal lesions and 100% of PEDs were located close (0–1 mm), upstream of the disc–fovea lines. Similarly, in the non-pachychoroid group, 77% of polypoidal lesions and 86% of PEDs were found in this location. No significant differences in lesion distribution were noted between the two groups (polypoidal lesions, $P = 0.580$; PEDs, $P = 0.223$). Notably, many non-pachychoroid PCV cases, classified using traditional macula-based criteria, demonstrated lesion distributions linked to vortex vein drainage areas, resembling those in pachychoroid PCV.

Investigative Ophthalmology & Visual Science

Discussion

This study examined the spatial distribution of polypoidal lesions and PEDs in eyes with PCV, analyzing widefield SS-OCT and B-scan images. Our findings revealed a strong correlation between lesion distribution and vortex vein characteristics, particularly the tendency of lesions to localize in upstream drainage areas of the dominant-side vortex veins, with no lesions in the opposite drainage area.

PCV, first reported by Yannuzzi et al. in 1982, is considered a subtype of neovascular AMD.[1,9,27] Unlike typical type 1 and 2 neovascular AMD, which results from the accumulation of drusen in the sub-RPE–basal lamina space and subsequent RPE dysfunction,[9,28] PCV presents distinct features. It is more prevalent in Asian populations than typical AMD[7,29] and shares similarities with CSC,[30] a representative pachychoroid spectrum disease. Recent studies have shown that eyes with PCV often exhibit characteristics such as dilation of macular vortex veins and CVH.[3,5,6,8,9,31,32] Mori et al.[33] suggested that genetic susceptibility to CSC and PCV may overlap; thus, it is possible that the basic pathology of PCV involves stasis or overload in the vortex veins, similar to CSC. However, a clear link between PCV and vortex vein characteristics has not been established.

Kishi et al.[18] reported that, in pachychoroid neovasculopathy, MNV tends to occur near the anastomosis of the superior and inferior vortex veins, as seen in widefield ICGA images. Kogo et al.[17] showed that, in CSC, PEDs and leak points tend to form around the upstream ends of dilated vortex veins. In our study, we observed that MNV in PCV similarly forms near the upstream ends of dilated vortex veins, particularly in eyes with asymmetric vortex veins. MNV was not observed in the non-dominant drainage area (Table 2), suggesting that CSC, pachychoroid neovasculopathy, and PCV may be related to pathologies within the same spectrum.

Peripapillary PCV occurs in 4.5% to 14.3% of Asian PCV cases and 18% to 75% of Caucasian cases.[32,34–39] However, its onset mechanism remains unclear. Baek et al.[34] reported localized choroidal thickening and dilation of Haller vessels near peripapillary lesions but not near the fovea. In our study, 6% of eyes exhibited peripapillary PCV, with lesions located around the upstream ends of vortex veins (Fig. 6). This suggests that disturbances in vortex vein blood flow may contribute to peripapillary PCV development, as seen in other types of PCV. Thus, distinguishing peripapillary PCV from others may not be necessary, as they likely share a common pathophysiology.

Pachychoroid PCV responds well to photodynamic therapy,[9,10] making it clinically valuable to classify PCV into pachychoroid or non-pachychoroid (driven by visible drusen) subtypes based on macular findings. Using previously reported methods, we classified the eyes analyzed in the present study into pachychoroid and non-pachychoroid subtypes and compared their characteristics. However, our analysis of using widefield SS-OCT images revealed that many eyes classified as non-pachychoroid had pachychoroid features such as lesions located upstream of vortex veins on the dominant side. This suggests that macular findings alone may not fully capture the pathogenesis of PCV.

Non-pachychoroid eyes displayed distinct characteristics compared to pachychoroid eyes, including a higher number of soft drusen in the macula and significantly thinner choroid both centrally and peripherally. In some non-pachychoroid cases, lesions were closer to the fovea, without a specific predilection for the vortex vein drainage areas. This suggests that, in some non-pachychoroid PCV cases, MNV may develop through mechanisms similar to pachychoroid PCV, driven by vortex vein blood flow disturbances, despite the presence of age-related drusen. These cases may represent pachychoroid features masked by drusen (Fig. 8). In other non-pachychoroid cases, MNV may arise independently, linked to soft drusen or pseudodrusen and associated RPE abnormalities (Fig. 8). These findings underscore the heterogeneity of PCV pathogenesis and the overlap between pachychoroid and drusen-related mechanisms. Assessing lesion location relative to vortex veins may help refine our understanding of the underlying pathology of each case, facilitating more tailored treatment, such as photodynamic therapy.

This study has several limitations: (1) We could not objectively assess PEDs of all sizes, as larger PED centers are

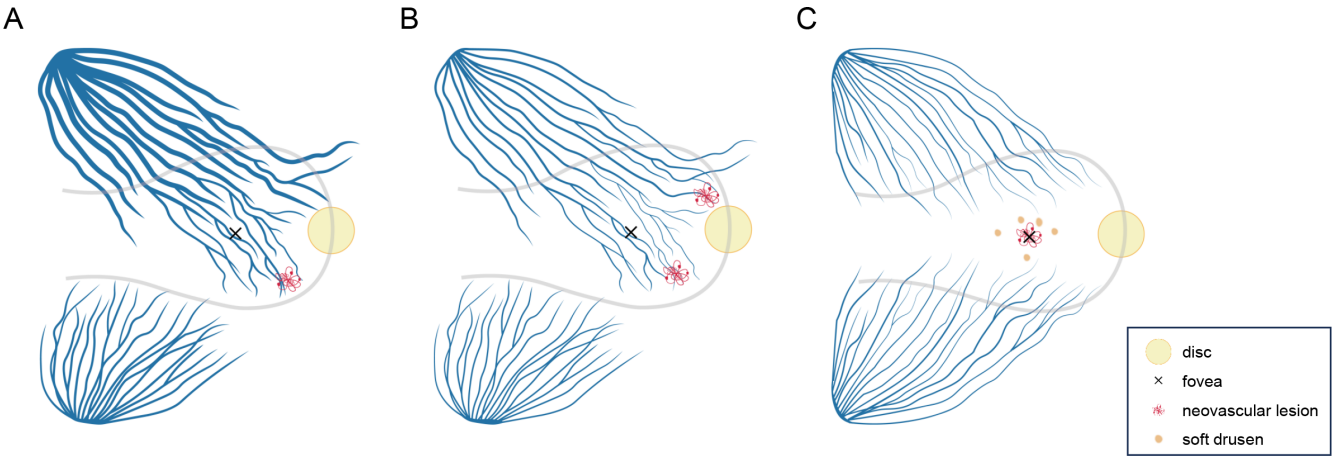

Figure 8. Schematic representation of the relationship between neovascular lesions and vortex veins in eyes with PCV. (**A**) Pachychoroidal PCV. Neovascular lesions occurred upstream of vortex veins, particularly in dilated (overloaded or stasis) veins. (**B**) Eyes without dilated choroidal veins in the macular area. Lesions occurred upstream of vortex veins and may extend beyond the fovea, displaying characteristics similar to those of pachychoroidal PCV cases. (**C**) Eyes with soft drusen. Lesions occurred near the fovea, regardless of vortex vein course, differing from the patterns seen in pachychoroidal PCV cases.

Investigative Ophthalmology & Visual Science

difficult to determine. (2) The study was cross-sectional, without longitudinal follow-up, because treatment strategies varied among cases. (3) The inclusion of only Japanese patients limits generalizability. (4) We did not assess the role of choroidal arteries and capillary systems in PCV pathogenesis. (5) We did not evaluate blood flow in neovascular lesions, as OCT angiography and ICGA have limitations, such as segmentation errors and artifacts; therefore, we used OCT B-scans to estimate the fibrovascular PED areas. (6) Distinguishing between fibrovascular and other types of PEDs (drusenoid, serous, and hemorrhagic) was sometimes challenging. (7) Although we used objective criteria to assess lesion locations, some assessments involved subjective judgment.

In conclusion, this study provides valuable insight into the relationship between vortex vein characteristics and neovascular lesions in PCV, aiding in more accurate diagnoses and treatment strategies. Future studies with larger samples, longitudinal follow-ups, and more comprehensive vascular assessments are necessary to validate and expand on these findings.

Acknowledgments

Supported in part by Canon (Tokyo, Japan). The funders had no role in the study design, data collection and analysis, decision to publish, or manuscript preparation.

Disclosure: **T. Kogo**, None; **Y. Muraoka**, Bayer Yakuhin (F), Novartis (F), Canon (F), Santen Pharmaceutical (F), Senju Pharmaceutical (F); **M. Hata**, Novartis (F), Senju Pharmaceutical (F), Kyoto Drug Discovery & Development (F); **M. Ishikura**, None; **N. Nishigori**, None; **Y. Akiyama**, None; **N. Ueda-Arakawa**, Santen Pharmaceutical (F), Novartis Pharma (F), Chugai Pharmaceutical (F); **M. Miyata**, Alcon Japan (F), Novartis (F), Santen Pharmaceutical (F), HOYA (F), Bayer Yakuhin (F), Senju Pharmaceutical (F), Kowa Pharmaceuticals (F); **S. Ooto**, Bayer Yakuhin (F), Novartis (F), Janssen Pharmaceuticals (F), Kowa Pharmaceuticals (F), AMO Japan (F), Santen Pharmaceutical (F), Alcon Japan (F), Senju Pharmaceutical (F); **A. Takahashi**, Bayer Yakuhin (F), Novartis (F), Santen Pharmaceutical (F), Merck (F); **M. Miyake**, Novartis (F), Bayer Yakuhin (F), Kowa Pharmaceuticals (F), Alcon Japan (F), AMO Japan (F), Santen Pharmaceutical (F), Senju Pharmaceutical (F), Johnson & Johnson (F), Chugai Pharmaceutical (F); **A. Tsujikawa**, Canon (F), Findex (F), Santen Pharmaceutical (F), Kowa Pharmaceuticals (F), Pfizer (F), AMO Japan (F), Senju Pharmaceutical (F), Wakamoto Pharmaceutical (F), Alcon Japan (F), Alconpharma (F), Otsuka Pharmaceutical (F), Tomey Corporation (F), Taiho Pharmaceutical (F), HOYA (F), Bayer Yakuhin (F), Novartis (F), Chugai Pharmaceutical (F), Astellas (F), Eisai (F), Daiichi-Sankyo (F), Janssen Pharmaceuticals (F), Kyoto Drug Discovery & Development (F), Allergan Japan (F), Merck (F), Ellex (F), Sanwa Kagaku Kenkyusho (F), Nitten Pharmaceutical (F), AbbVie (F)

References

1. Cheung CMG, Lai TYY, Teo K, et al. Polypoidal choroidal vasculopathy: consensus nomenclature and non-indocyanine green angiograph diagnostic criteria from the Asia-Pacific ocular imaging society PCV workgroup. *Ophthalmology*. 2021;128(3):443–452.
2. Imamura Y, Engelbert M, Iida T, Freund KB, Yannuzzi LA. Polypoidal choroidal vasculopathy: a review. *Surv Ophthalmol*. 2010;55(6):501–515.
3. Cai C-X, Xiong X-M, Li T, et al. Vortex vein engorgement and different shapes of venous drainage systems in polypoid choroidal vasculopathy vs. age-related macular degeneration on indocyanine green angiography. *Exp Ther Med*. 2023;25(4):162.
4. Funatsu R, Sonoda S, Terasaki H, et al. Choroidal morphologic features in central serous chorioretinopathy using ultra-widefield optical coherence tomography. *Graefes Arch Clin Exp Ophthalmol*. 2023;261(4):971–979.
5. Jeong A, Lim J, Sagong M. Choroidal vascular abnormalities by ultra-widefield indocyanine green angiography in polypoidal choroidal vasculopathy. *Invest Ophthalmol Vis Sci*. 2021;62(2):29.
6. Matsumoto H, Hoshino J, Arai Y, et al. Quantitative measures of vortex veins in the posterior pole in eyes with pachychoroid spectrum diseases. *Sci Rep*. 2020;10(1):19505.
7. Matsumoto H, Hoshino J, Mukai R, Nakamura K, Kishi S, Akiyama H. Clinical characteristics and pachychoroid incidence in Japanese patients with neovascular age-related macular degeneration. *Sci Rep*. 2022;12(1):4492.
8. Mukai R, Itagaki K, Honjyo J, Matsumoto H, Sekiryu T. Relationship between pulsation of posterior vortex vein, choroidal thickness, and choroidal vascular hyperpermeability in polypoidal choroidal vasculopathy. *Graefes Arch Clin Exp Ophthalmol*. 2023;261(12):3475–3480.
9. Yamashiro K, Yanagi Y, Koizumi H, et al. Relationship between pachychoroid and polypoidal choroidal vasculopathy. *J Clin Med*. 2022;11(15):4614.
10. Hata M, Tagawa M, Oishi A, et al. Efficacy of photodynamic therapy for polypoidal choroidal vasculopathy associated with and without pachychoroid phenotypes. *Ophthalmol Retina*. 2019;3(12):1016–1025.
11. Imanaga N, Terao N, Sawaguchi S, et al. Clinical factors related to loculation of fluid in central serous chorioretinopathy. *Am J Ophthalmol*. 2022;235:197–203.
12. Lehmann M, Wolff B, Vasseur V, et al. Retinal and choroidal changes observed with "en face" enhanced-depth imaging OCT in central serous chorioretinopathy. *Br J Ophthalmol*. 2013;97(9):1181–1186.
13. Matsumoto H, Hoshino J, Mukai R, et al. Vortex vein anastomosis at the watershed in pachychoroid spectrum diseases. *Ophthalmol Retina*. 2020;4(9):938–945.
14. Spaide RF, Gemmy Cheung CM, Matsumoto H, et al. Venous overload choroidopathy: a hypothetical framework for central serous chorioretinopathy and allied disorders. *Prog Retin Eye Res*. 2022;86:100973.
15. Terao N, Imanaga N, Wakugawa S, et al. Ciliochoroidal effusion in central serous chorioretinopathy. *Retina*. 2022;42(4):730–737.
16. Ishikura M, Muraoka Y, Nishigori N, et al. Widefield choroidal thickness of eyes with central serous chorioretinopathy examined by swept-source OCT. *Ophthalmol Retina*. 2022;6(10):949–956.
17. Kogo T, Muraoka Y, Ishikura M, et al. Pigment epithelial detachment and leak point locations in central serous chorioretinopathy. *Am J Ophthalmol*. 2024;261:19–27.
18. Kishi S, Matsumoto H. A new insight into pachychoroid diseases: remodeling of choroidal vasculature. *Graefes Arch Clin Exp Ophthalmol*. 2022;260(11):3405–3417.
19. Hirano M, Muraoka Y, Kogo T, et al. Analysis of widefield choroidal thickness maps of healthy eyes using swept source optical coherence tomography. *Sci Rep*. 2023;13(1):11904.
20. Nishigori N, Muraoka Y, Ishikura M, et al. Extensive reduction in choroidal thickness after photodynamic therapy in eyes with central serous chorioretinopathy. *Sci Rep*. 2023;13(1):10890.
21. Hiroe T, Kishi S. Dilatation of asymmetric vortex vein in central serous chorioretinopathy. *Ophthalmol Retina*. 2018;2(2):152–161.

22. Hayreh SS. Segmental nature of the choroidal vasculature. *Br J Ophthalmol*. 1975;59(11):631–648.
23. Bennett AG, Rudnicka AR, Edgar DF. Improvements on Littmann's method of determining the size of retinal features by fundus photography. *Graefes Arch Clin Exp Ophthalmol*. 1994;232(6):361–367.
24. Kadomoto S, Muraoka Y, Ooto S, et al. Evaluation of macular ischemia in eyes with branch retinal vein occlusion: an optical coherence tomography angiography study. *Retina*. 2018;38(2):272–282.
25. Spaide RF. Disease expression in nonexudative age-related macular degeneration varies with choroidal thickness. *Retina*. 2018;38(4):708–716.
26. Takahashi A, Hosoda Y, Miyake M, et al. Clinical and genetic characteristics of pachydrusen in eyes with central serous chorioretinopathy and general Japanese individuals. *Ophthalmol Retina*. 2021;5(9):910–917.
27. Ciardella AP, Donsoff IM, Huang SJ, Costa DL, Yannuzzi LA. Polypoidal choroidal vasculopathy. *Surv Ophthalmol*. 2004;49(1):25–37.
28. Voichanski S, Bousquet E, Abraham N, et al. En face optical coherence tomography illustrates the trizonal distribution of drusen and subretinal drusenoid deposits in the macula. *Am J Ophthalmol*. 2024;261:187–198.
29. Maruko I, Iida T, Saito M, Nagayama D, Saito K. Clinical characteristics of exudative age-related macular degeneration in Japanese patients. *Am J Ophthalmol*. 2007;144(1):15–22.
30. Kido A, Miyake M, Tamura H, et al. Incidence of central serous chorioretinopathy (2011–2018): a nationwide population-based cohort study of Japan. *Br J Ophthalmol*. 2022;106(12):1748–1753.
31. Chung SE, Kang SW, Kim JH, Kim YT, Park DY. Engorgement of vortex vein and polypoidal choroidal vasculopathy. *Retina*. 2013;33(4):834–840.
32. Koizumi H, Yamagishi T, Yamazaki T, Kawasaki R, Kinoshita S. Subfoveal choroidal thickness in typical age-related macular degeneration and polypoidal choroidal vasculopathy. *Graefes Arch Clin Exp Ophthalmol*. 2011;249(8):1123–1128.
33. Mori Y, Miyake M, Hosoda Y, et al. Genome-wide survival analysis for macular neovascularization development in central serous chorioretinopathy revealed shared genetic susceptibility with polypoidal choroidal vasculopathy. *Ophthalmology*. 2022;129(9):1034–1042.
34. Baek J, Dansingani KK, Lee JH, Lee WK, Freund KB. Choroidal morphology in eyes with peripapillary polypoidal choroidal vasculopathy. *Retina*. 2019;39(8):1571–1579.
35. Hou J, Tao Y, Li XX, Zhao MW. Clinical characteristics of polypoidal choroidal vasculopathy in Chinese patients. *Graefes Arch Clin Exp Ophthalmol*. 2011;249(7):975–979.
36. Kwok AK, Lai TY, Chan CW, Neoh EL, Lam DS. Polypoidal choroidal vasculopathy in Chinese patients. *Br J Ophthalmol*. 2002;86(8):892–897.
37. Spaide RF, Yannuzzi LA, Slakter JS, Sorenson J, Orlach DA. Indocyanine green videoangiography of idiopathic polypoidal choroidal vasculopathy. *Retina*. 1995;15(2):100–110.
38. Wen F, Chen C, Wu D, Li H. Polypoidal choroidal vasculopathy in elderly Chinese patients. *Graefes Arch Clin Exp Ophthalmol*. 2004;242(8):625–629.
39. Yannuzzi LA, Ciardella A, Spaide RF, Rabb M, Freund KB, Orlock DA. The expanding clinical spectrum of idiopathic polypoidal choroidal vasculopathy. *Arch Ophthalmol*. 1997;115(4):478–485.

Investigative Ophthalmology & Visual Science